Visible Cloud Imager for Autonomous Telescopes

W. Jody Mandeville, Tim McLaughlin, Steve Bygren, Christian Randell
The MITRE Corporation

CONFERENCE PAPER

This paper describes the implementation of a commercially available, visible all-sky camera as a cloud detector for an autonomous network of small telescopes. The detected location of clouds is used to allow real-time optimization of scheduled observations. A simplified numeric method for mapping pixel location in the image to azimuth and elevation is detailed.

1. INTRODUCTION

With the proliferation of autonomous small telescope networks, it is desirable to have a cloud detector that can be used to reduce time spent attempting to collect data when transient clouds are obscuring portions of the sky. The conventional method of cloud detection for a small telescope is to use a Boltwood Cloud Sensor or similar device. This type of device measures the amount of cloud cover by comparing the temperature of the sky to the ambient ground level temperature, where a large temperature difference between the sky and the ground level indicates clear skies. This sky temperature measurement is based on a single IR detector sensing the average temperature of the entire sky. The Air Force's Ground-based Electro-Optical Deep Space Surveillance (GEODSS) system employs a much more capable Infrared Cloud Imager (IRCI) for the purpose of cloud detection. IRCI uses the same IR temperature measurement technique as a Boltwood-type device but does so with an array of sensors dividing the sky into 104 zones.[1] This allows the GEODSS telescopes to continue to operate efficiently during partially clouded nights by adjusting the observation schedule to not look in sectors where clouds have been detected. Just like the Air Force's GEODSS system, an autonomous network of small telescopes would benefit from a device capable of monitoring and reporting cloud cover by sector. IRCI is a complex and costly solution, so we chose to implement a commercial off-the-shelf (COTS) visible all-sky camera to perform a similar function.

In this paper we investigate the calibration and implementation of our Visible Cloud Imager (VCI) which was designed to be used in conjunction with our autonomous network of small telescopes. The purpose of the all-sky camera described here is to detect the location of transient clouds which can then be used to modify the schedule of observations. The Background section discusses how we calibrate our all-sky camera pixel locations to celestial azimuth and elevation. Our approach has the advantage of being able to compensate for distortions that are difficult to model, to include imperfections in the plexiglass dome protecting the camera. In the Results/Discussion section we present the performance of our cloud detection algorithm.

2. BACKGROUND

The all-sky camera lens is protected from the environment by a plexiglass dome. This dome adds random distortions that are not accounted for in the published calibration techniques for fisheye lenses[2][3][5]. We correct for this by combining a simple fisheye projection model with a numerical calibration technique. Our analytic model is based on a the following equation that converts an object point for an equidistant fisheye lens to its rectilinear equivalent[4]:

$$r_d = f \arctan(\frac{r_u}{f}), \tag{1}$$

where r_u is the undistorted length from the optical axis, r_d is the distorted length from the optical axis, and f is the effective focal length. After correcting for the gross distortion, we then correct for the remaining minor distortions, including imperfections in the plexiglass dome and atmospheric refraction, by measuring

residuals between our detected star locations and the modeled locations. The magnitudes of the residuals are mapped and smoothed across the focal plane. This mapping provides a final correction for our calibration.

To calibrate a camera, we start by taking a ten second image on a clear night and employ a modified Random Sample Consensus (RANSAC)[6] technique. We randomly select five stars and optimize the model coefficients for the best residuals between the detected position and the position we calculate using Equation 1. We then score that candidate solution against all stars that should be visible to our camera ($V_{mag} < 5.5$). This process is repeated several times with each new candidate solution being scored. The candidate solution with the best score is used as the rough calibration solution. Next we map out the residuals between our rough calibration solution and the actual star locations across the entire image, and use this residual map as a fine adjustment for our final calibration.

Once we have calibrated our all-sky camera, we can use it to determine when a star is not detected that has a high enough signal-to-noise ratio to have been detected in a dark, cloudless sky. When these stars are not detected, this is an indication of a cloud or some other obscuration. To map the clouded regions, we divide the sky into 104 zones and determine how obscured each zone is by the number of missing stars in each region. The number of zones is arbitrary, so we choose to use the same number as is used by the Air Force's IRCI.[1] For diagnostics and real-time operator view, the cloud conditions can be displayed on a cloud map using a graduated color scale with red indicating a zone that is totally obscured and green indicating a zone that is totally clear. The observation scheduling software can use the current sky conditions to optimize observation time by not spending time trying to collect data in zones that are obscured more than a threshold value determined by operational considerations.

3. RESULTS/DISCUSSION

We tested our visible cloud imager during various cloud cover conditions to see how it performed. Our test site is located thirty miles east of the greater metropolitan area of Colorado Springs, Colorado, which is a significant source of light polution. Fig. 1 shows the performance during a clear, cloudless night. The left image is the picture from the all-sky camera. On the corresponding cloud map to the right, the majority of the sectors are green, which indicates that nearly all of expected stars are detected across the sky. A few sectors to the east are depicted as red/orange because they are obscured by a telescope dome where no stars can be detected. To the west the sectors are yellow/orange because the city glow is preventing the detection of some of the stars. A night with complete cloud cover is shown in Fig. 2. The associated cloud map shows all red/orange sectors indicating few stars are detected at the expected locations. Consequently from this data we would conclude that there are no zones acceptable for observations. Fig. 3 shows partial cloud cover. The image on the left shows stars from zenith to the northwest. The associated cloud map shows good agreement with the zones from zenith to the northwest colored green.

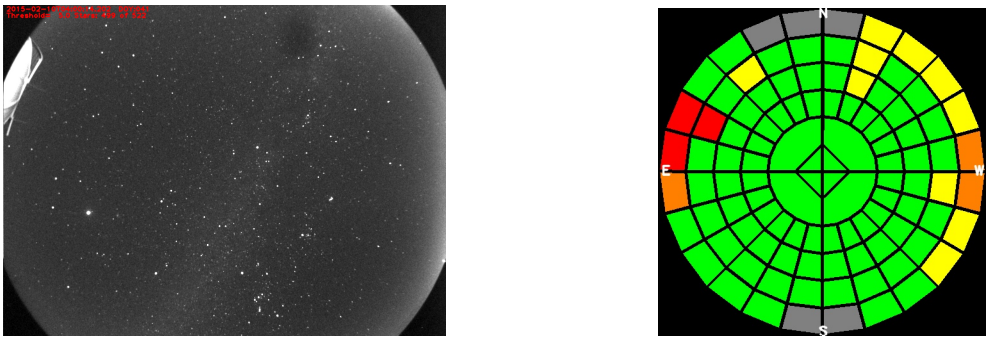

Figure 1: Images show results with no cloud cover. Notice the telescope dome to the east obscures four zones in the associated cloud map indicating an area where stars are obscured. Additionally there are some obscured zones near the western horizon due to the city glow of Colorado Springs.

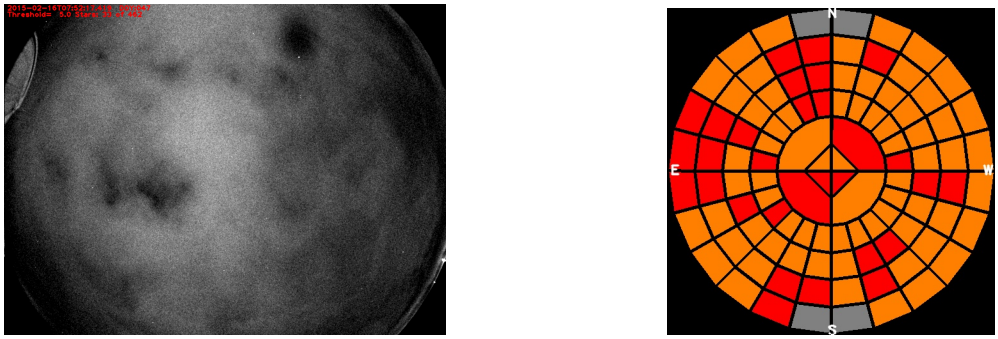

Figure 2: Images show results with complete cloud cover. No zones are available for reliable data collection.

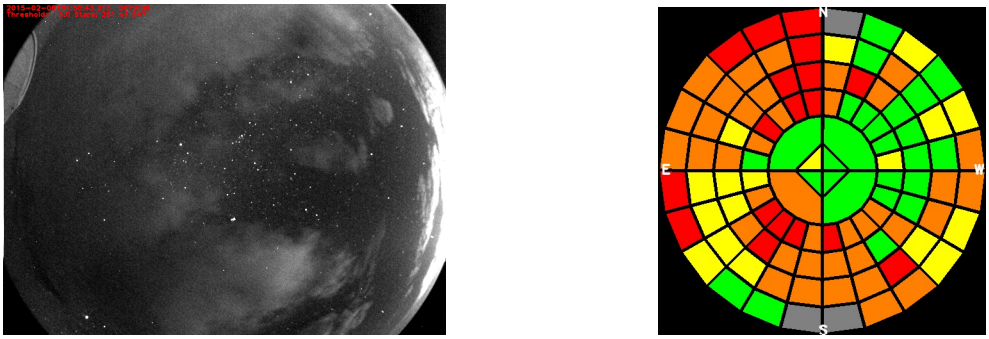

Figure 3: Images show results with partial cloud cover. The regions that are green or yellow are locations where the sky is clear enough for the scheduling routine to attempt to collect data.

Additional testing was performed during nights with a bright moon. Fig. 4 shows a time when there was a large moon to the southeast. For display purposes we have integrated an electronic moon block that shows up as the black circle covering the moon. The moon block prevents the display software from automatically adjusting the scaling and washing out the stars. The orange and yellow zones to the west are due to the city glow from Colorado Springs. The number of zones impacted by the city glow when there is a moon in the sky is larger than when there is no moon in the sky (compare to Fig. 1). The additional obscured zones are a result of the additive effect of the moon in combination with the city glow. Fig. 5 shows a partly cloudy sky with a large moon to the south. Good viewing conditions are indicated by the green sectors to the north and east.

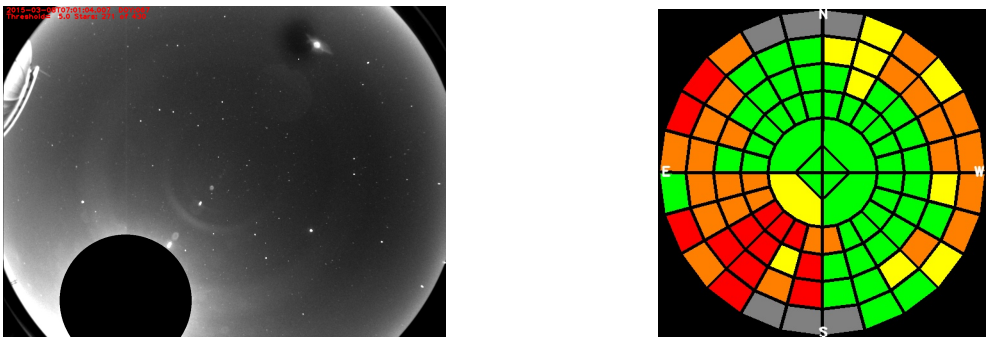

Figure 4: Images show a clear night with a near full moon to the southeast. The cloud map shows red where the moon is obscuring stars as expected. Aditional red sectors appear to the west as a result of city glow from Colorado Springs.

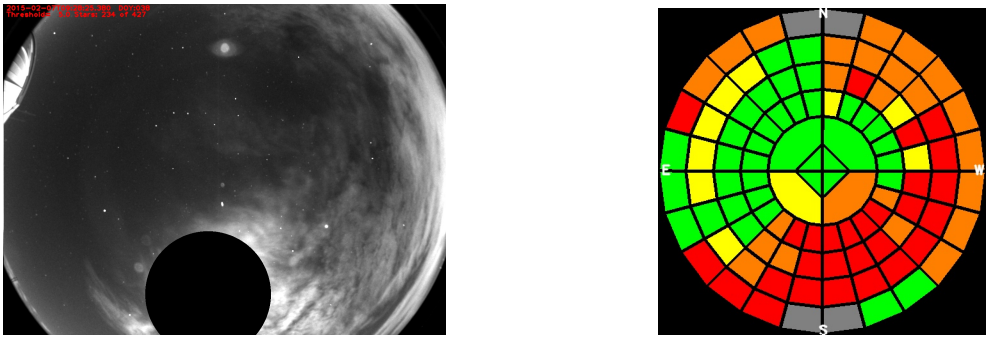

Figure 5: Images show a partly cloudy night with a near full moon to the south. The cloud map shows red where the moon is obscuring stars as expected.

An additional feature of VCI is the ability to record the amount of cloud cover as a function of time. Fig. 6 shows a full night of data. At the beginning of the night no stars were detected since the sky was too bright. Following twilight, the percentage of detected stars climbed to over 80% of the expected number of stars. The missing stars are likely from the western horizon where they are obscured by city glow. Later in the night clouds rolled in, which is indicated by the drop in detected stars as well as the increased red in the cloud maps.

Our scheduling software is designed to modify the order of observations based on current cloud conditions. Fig. 7 shows a screenshot from VCI on the left with a yellow circle indicating the location of Vega which is where the telescope is pointed. The right image is a screenshot of our telescope control program (SkyX) pointing our telescope at Vega which is currently unobscured by clouds.

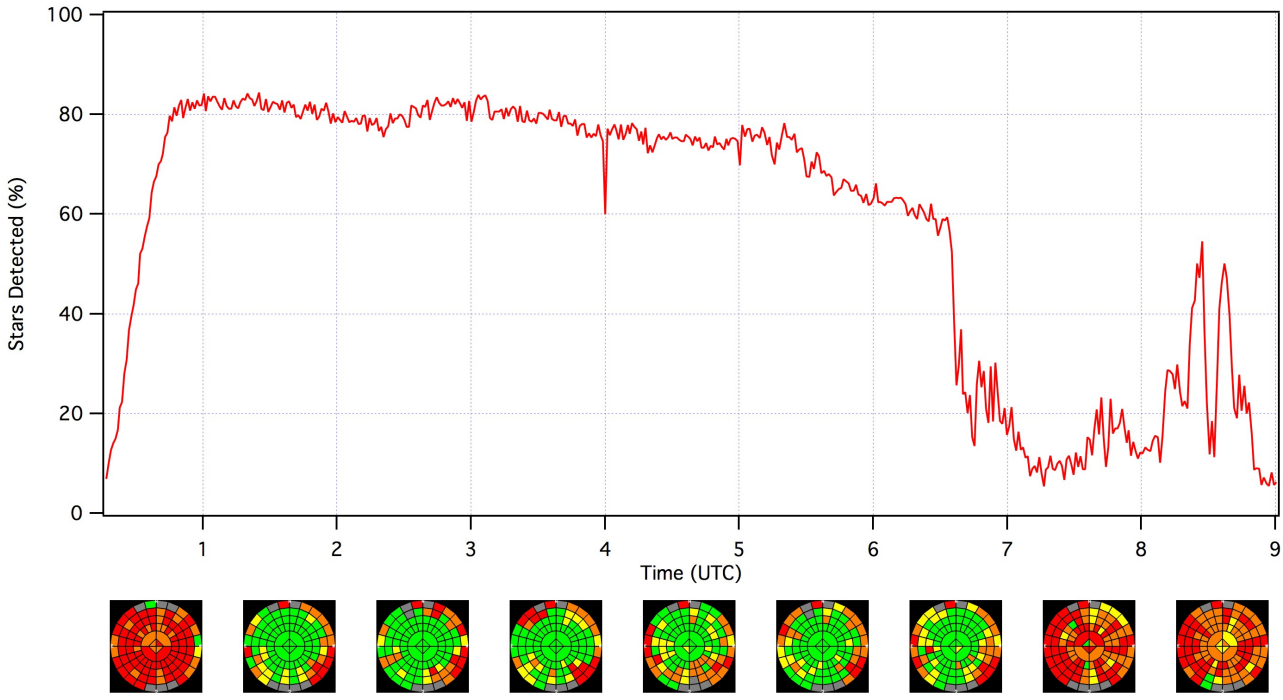

Figure 6: Graph shows the percentage of stars that are detected as a function of time throughout a full night. The thumbnails show some of the associated cloud maps.

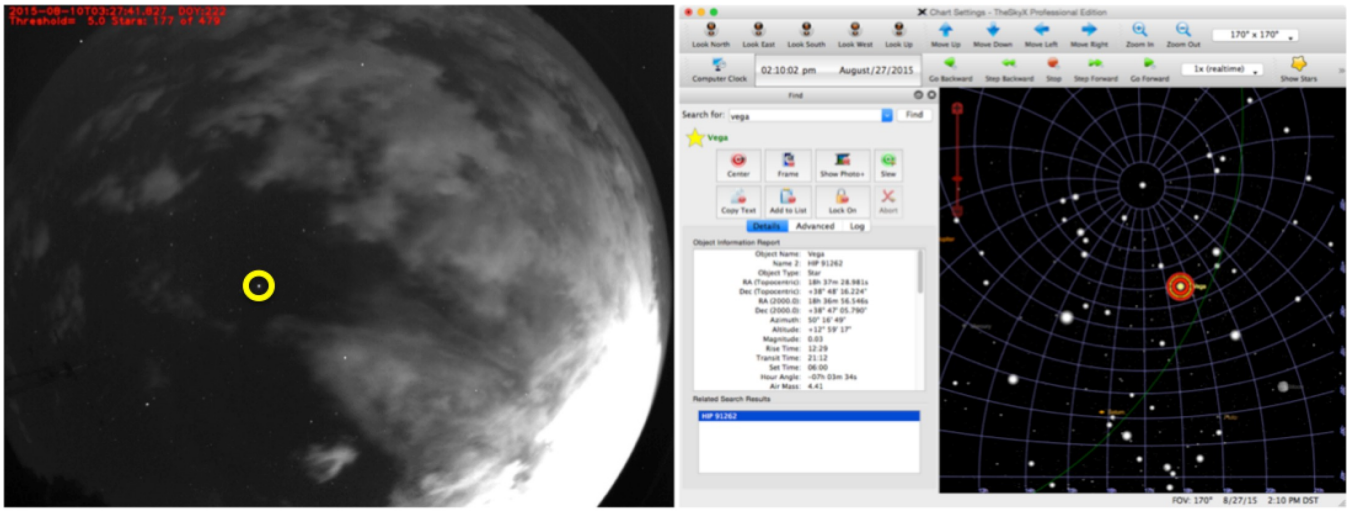

Figure 7: All-sky image on the left shows a yellow circle around Vega which is in a clear portion of a partly cloudy sky. The right image shows the corresponding screenshot from our telescope control software (SkyX).

4. CONCLUSION

We have successfully developed a Visible Cloud Imager capable of being used to report not only the amount of cloud cover but the position of the clouds. VCI can be used to optimize our observing schedules. Additional benefits come from VCI identifying other sources of obscurations including physical structures, city glow, and the moon, which would not be detected based on temperature measurements, a benefit over infrared based systems. VCI provides the small telescope community a low-cost solution for cloud location determination.

We would like to thank the SMC/SYGO and the United States Air Force Academy for continued collaboration and support. Additionally we would like to acknowledge the funding provided by MITRE's internal research program.

This technical data was produced for the U.S. Government under Contract No. FA8702-15-C-0001, and is subject to the Rights in Technical Data-Noncommercial Items Clause (DFARS) 252.227-7013 (NOV 1995).

5. REFERENCES

[1] GDS-D-SPM-0900 Revision A. Technical report, GEODSS Program Office, 2014.

[2] Steven M. Bannister. New calibration technique for all sky cameras. Master's thesis, New Mexico State University, Las Cruces, New Mexico, December 2012.

[3] J Borovicka, P Spurny, and J Keclikova. A new positional astrometric method for all-sky cameras. *Astronomy and Astrophysics Supplement Series*, 112:173, 1995.

[4] Ciaran Hughes, Edward Jones, and Martin Glavin. Simple fish-eye calibration method with accuracy evaluation. In *ELCVIA: electronic letters on computer vision and image analysis*, volume 10, pages 0054–62, 2011.

[5] Ellen Schwalbe. Geometric modelling and calibration of fisheye lens camera systems. In *Proc. 2nd Panoramic Photogrammetry Workshop, Int. Archives of Photogrammetry and Remote Sensing*, volume 36, page W8, 2005.

[6] Marco Zuliani. Ransac for dummies. *Vision Research Lab, University of California, Santa Barbara*, 2009.